Synthesis and Photovoltaic Properties of Two Benzo[1,2-*b*:3,4-*b*′]dithiophene-Based Conjugated Polymers

Jianhui Hou,* Hsiang-Yu Chen, Shaoqing Zhang, and Yang Yang*

Department of Materials Science and Engineering & California Nanosystems Institute, University of California Los Angeles, Los Angeles, California 90095

Received: June 28, 2009; Revised Manuscript Received: November 03, 2009

Side chains of conjugated polymers play an important role in their properties. To investigate the influence of side chains on photovoltaic properties, two conjugated polymers with benzo[1,2-*b*:3,4-*b*]dithiophene (BDT) and 4,7-dithiophen-2,1,3-benzothiadiazole (DTBT) units, **Z3** and **Z4**, were designed and synthesized. These two polymers have identical conjugated main chains and very similar side chains. In polymer **Z3**, hexyl groups are linked to the thiophene units directly, and in polymer **Z4**, hexyloxy groups are linked to the thiophene units. Since the hexyloxy group exhibits a smaller steric hindrance and a stronger electron donating effect than the hexyl group, properties of **Z3** and **Z4** are very different. The hole mobility of the **Z3**:PCBM blend film is 1.84×10^{-7} cm^2/(V s), which is 2 orders lower than that of the **Z4**:PCBM blend, and photovoltaic results demonstrate that the fill factor (FF) of the **Z3**-based device is 0.37, while that of the **Z4**-based polymer solar cell (PSC) device reached 0.61. These results reveal that steric hindrance of the side chain is an important issue for a new material design, in order to obtain higher FF. Additionally, thermal stability, absorption spectra, electrochemical, PL quenching of the polymer:PCBM blend, and photovoltaic properties of the two polymers were investigated in detail. For **Z3**-based devices, a power conversion efficiency (PCE) of ~2% was observed with an open circuit voltage (V_{oc}) of 0.84 V, a short circuit current (J_{sc}) of 6.3 mA/cm^2, which indicates this kind of conjugated polymer should be a promising material in the application of polymer solar cells.

Introduction

Since the discovery of photoinduced charge transfer in composites of conjugated polymers and C_{60},[1] polymer solar cells (PSCs) have attracted considerable attention because of their potential for use in low-cost, lightweight, solution-processable, and flexible large area panels.[2−5] As the electron donor material in the active layer of PSC devices, properties of conjugated polymers, such as absorption spectra, molecular energy levels, carrier mobility, etc., have great influence on the photovoltaic performance of devices. For example, as reported, the highest J_{sc} of the PSC devices based on poly(3-hexylthiophene) (P3HT) was 10.7 mA/cm^{-2}, due to the absorption range limitation of the active layer materials,[6] To get a better response range of PSC device and hence higher J_{sc}, smaller bandgap conjugated polymers were applied to PSCs.[7] In these works, poly[4,4-bis(2-ethylhexyl)cyclopenta[2,1-*b*;3,4-*b*′]dithiophene-*alt*-2,1,3-benzothiadiazole] (PCPDTBT) is one of the most successful small bandgap polymers for application of PSC. The absorption range of the PSC devices based on PCPDTBT was extended from 650 nm to around 850 nm. As a result, the J_{sc} of the PSC device reached 16.2 mA/cm^{-2} after optimizing the morphology. The highest occupied molecular orbital (HOMO) level of conjugated polymers is another important issue of their photovoltaic properties.[8] For instance, although the bandgap of poly[(2,7-silafluorene)-*alt*-(4,7-di-2-thienyl-2,1,3-benzothiadiazole)] (PSiFDBT) is similar to that of P3HT, this material exhibits a much lower HOMO level than P3HT. As a result, the V_{oc} of the PSiFDBT-based PSC devices reached 0.9 V, which is much higher than that of P3HT-based devices. With such high V_{oc}, an efficiency of 5.4% has been achieved by using PSiFDBT as the active layer material.[10]

Recently, several models were proposed to estimate photovoltaic properties of conjugated polymers,[8,11,12] and these works provided valuable guidelines for conjugated polymer molecular structure design. As proposed, both molecular energy level and bandgap are of the most importance for obtaining highly efficient PSCs. There are many works focusing on optimizing bandgap and molecular energy level by changing the molecular structure of conjugated polymers. For example, Luping et al. reported a systematic work about the design of thieno[3,4-*b*]thiophene-based conjugated polymers for solar cells, and in that work, several conjugated polymers with ideal bandgap and energy level were designed and synthesized, and also a PCE of 6.1% has been achieved.[9] Although the results from PSC devices indicate that these polymers are promising photovoltaic materials, performances of these materials are much lower than the theoretical value as expected from their bandgap and energy level values. The deviation reveals that photovoltaic properties of conjugated polymers are not solely determined by the

SCHEME 1: Molecular Structures of Polymers Z3 and Z4

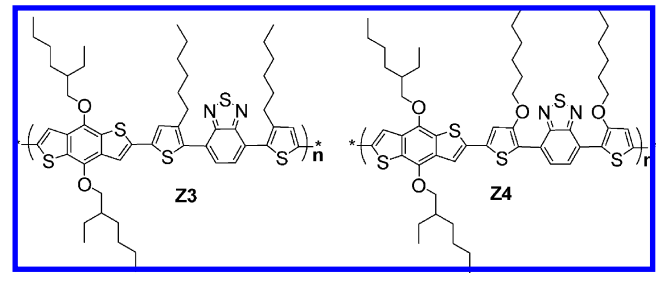

* To whom correspondence should be addressed. E-mail: jhhou@ucla.edu and yangy@ucla.edu.

10.1021/jp9060413

SCHEME 2: Synthetic Procedures of Polymers Z3 and Z4[a]

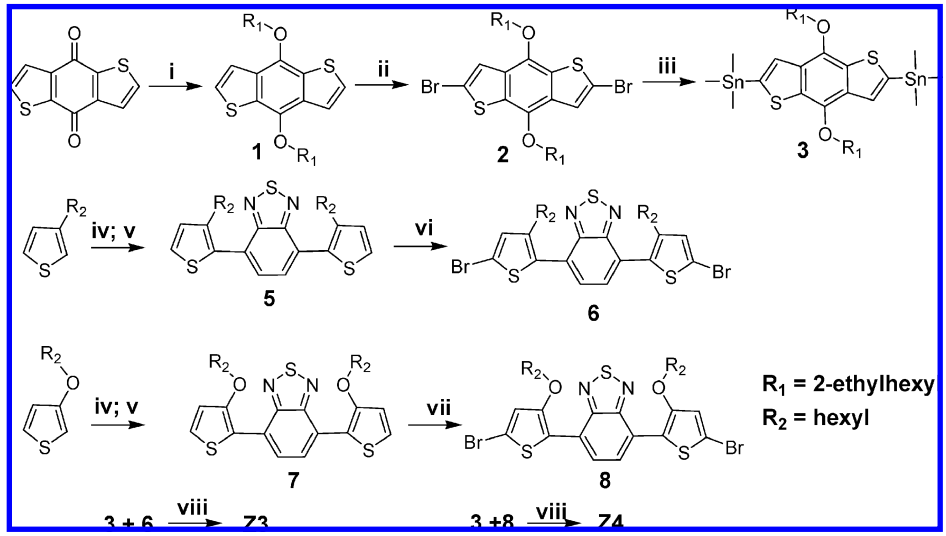

[a] Reagents and conditions: (i) Zn, NaOH, H_2O, reflux for 1 h; then *i*-$C_8H_{17}Br$, TBAB, reflux for 6 h; (ii) Br_2, methylene chloride, ambient temperature, 4−6 h; (iii) *n*-butyllithium, THF, −78 °C, 1 h; then ambient temperature for 1 h, and then $(CH_3)_3SnCl$, ambient temperature, 2 h, argon; (iv) *n*-butyllithium, THF, −78 °C, 1 h; then ambient temperature for 1 h, and then $(C_4H_9)_3SnCl$, ambient temperature, 2 h, argon; (v) 4,7-dibromo-2,1,3-benzothiadiazole, toluene, $Pd(PPh_3)_4$, reflux for 16 h; (vi) NBS, chloroform, ambient temperature, overnight; (vii) NBS, chloroform, 4 °C for 1 h; then ambient temperature overnight; (viii) $Pd(PPh_3)_4$, toluene, reflux for 24 h.

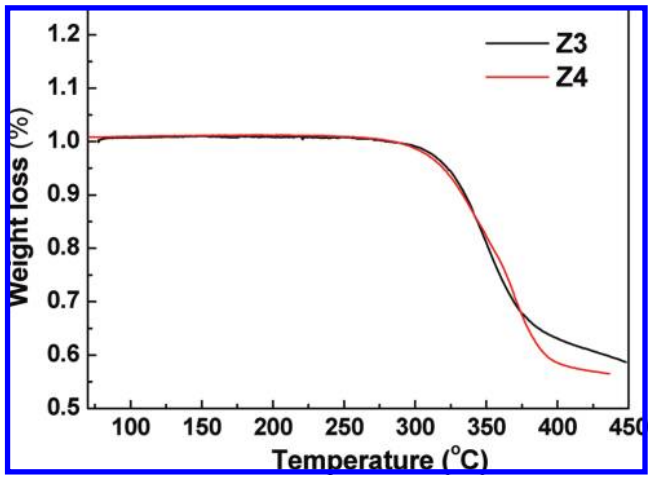

Figure 1. TGA plots of **Z3** and **Z4** with a heating rate of 10 deg/min in the air.

bandgap and energy level of the materials. Besides the bandgap and molecular energy level, some other properties, such as mobility and solubility, are also important to photovoltaic polymers. As known, these properties of conjugated polymers are more susceptible to molecular structures, such as regioregularity, orientation, or steric hindrance between repeated units. So, side chains of conjugated polymers play an important role in their photovoltaic properties. However, the influence of side chains of conjugated polymers on their photovoltaic properties is less reported. There is a great need for investigation and understanding of the side chain effects. Recently, we reported a family of benzo[1,2-*b*;3,4-*b*]dithiophene (BDT)-based conjugated polymers with promising photovoltaic properties,[13] and in order to modify bandgap and molecular energy levels, BDT was copolymerized with different conjugated units. In this work, two polymers with BDT units, **Z3** and **Z4** in Scheme 1, were designed and synthesized in order to investigate the influence of side chains on their photovoltaic properties.

Synthesis of the Polymers. Synthesis routes of the two polymers were shown in Scheme 2. 2,6-Bis(trimethyltin)-4,8-bis(2-ethylhexoxy)benzo[1,2-*b*;3,4-*b*]dithiophene, compound **3**, was synthesized by a similar method reported in our previous work,[13] and purified by recrystallization with ethyl alcohol as solvent. Both polymers were prepared by Stille coupling reaction with good yield. The number average molecular weight (M_n) of **Z3** and **Z4** is 23.2K and 19.2K, with a PDI of 1.3 and 1.2, respectively.

Thermal Stability. These two polymers exhibited very similar thermal stability, as shown in the thermogravimetric analysis (TGA) plots of **Z3** and **Z4** in Figure 1. The onset decomposition temperatures of the polymers are around 280 °C in air, mainly due to the leaving of alkoxy groups. The thermal stability of these two polymers is adequate for their applications in PSCs and other optoelectronic devices.

Absorption Spectra of the Polymers. Absorption spectra of polymer **Z3** and **Z4** are shown in Figure 2, and some data from this figure were summarized in Table 1 for comparison. On the basis of the onset point of the absorption spectrum, the optical bandgap of **Z4** was estimated to be about 1.55 eV, which is 0.27 eV lower than that of **Z3**. The lower bandgap of **Z4** than **Z3** should be attributed to the strong electron-donating effect of the alkyoxy groups on **Z4**. As shown in Figure 2, both polymers exhibit two absorption peaks in the UV−vis region. In comparison with the absorption spectra in chloroform, absorption spectra of the polymer thin films shift to a longer wavelength region. Polymer **Z3** exhibits a red shift of ∼51 nm while that of **Z4** is only ∼8 nm. It is known that the absorption spectra of conjugated polymers closely relate to their effective conjugated length, which is susceptible to the steric hindrance caused by side chains. For example, the absorption spectrum of the regiorandom poly(3-hexylthiophene) film exhibits a peak at around 500 nm, but the absorption peak of the poly(3-cyclohexylthiophene) film is at 410 nm due to the strong steric hindrance caused by the cyclohexyl groups.[14] As shown in Scheme 1, hexyl side chains of **Z3** are linked to thiophene units directly; for **Z4**, they are linked to thiophene units through oxygen atoms. For both **Z3** and **Z4**, there is no substituent on the 3 and 7 positions of the BDT units and the 4 position of the thiophene units, so the steric hindrance effects between BDT

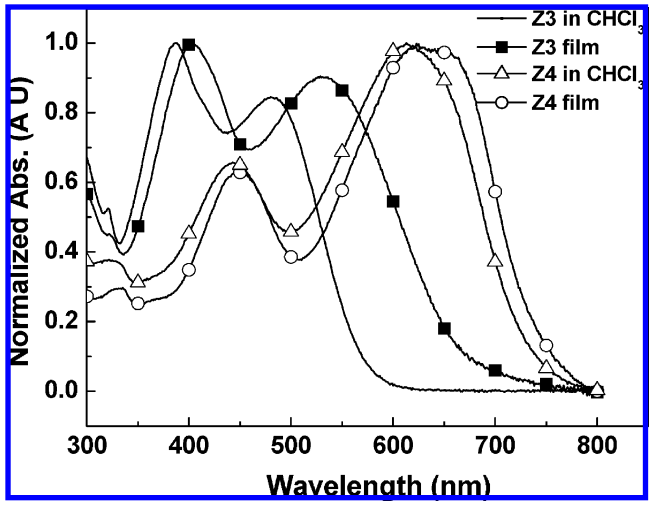

Figure 2. Absorption spectra of polymers **Z3** and **Z4** as films and in chloroform.

TABLE 1: Optical Properties and HOMO Level Values of Z3 and Z4

	λ_{max} (nm) soln/film	soln/film	E_g (eV)	E_{ox} (V)/HOMO (eV)
Z3	387/404	480/531	1.85	0/−4.80
Z4	443/451	613/625	1.55	0.40/−5.2

units and thiophene units of the two polymers are very similar. As a result, the steric hindrance between the thiophene and the 2,1,3-benzothiadiazole (BT) should play a more important role here. As reported, in polythiophenes, the alkyl group exhibits bigger steric hindrance to the adjacent units than the alkoxy group,[15] and therefore, in comparison with **Z3**, more planar structure will be formed in **Z4**, in both solution state and solid state. As shown in Figure 2, the **Z3** film has a larger red-shift in absorption compared to its solution than that of **Z4**. This means that the steric hindrance in **Z3** caused by its side chain is bigger than that of **Z4**. Consequently, a more plane structure of the main chain and hence a more effective interchain $\pi-\pi^*$ stacking could be formed in the polymer **Z4**. So, it can be expected that **Z4** has a higher mobility than **Z3**.

Electrochemical Properties. Electrochemical cyclic voltammetry (CV) is often performed for determining the HOMO level of conjugated polymers.[16] Figure 3 shows the CV curves of **Z3** and **Z4** films on the Pt electrode in 0.1 mol/L, Bu_4NPF_6, CH_3CN solution. It can be seen that there are reversible p-doping/dedoping (oxidation/rereduction) processes for both polymers. The onset of the p-doping process of **Z3** is 0.43 V, corresponding to a HOMO level of −5.23 eV, which is 0.4 eV lower than that of **Z4**. The strong electron-donating effect of the alkoxy groups of **Z4** should be the main reason for the higher HOMO level of **Z4**, which indicates that although alkoxy is a very effective functional group to reduce bandgap, it is not a good choice for lowering the bandgap of photovoltaic materials, because a deeper HOMO level is crucial to obtain a high V_{oc}.

Photovoltaic Properties. Figure 4 shows the $I-V$ curves of the PSCs with **Z3**:PCBM and **Z4**:PCBM as active layer materials, and the results of the devices were collected in Table 2. From these results, we found that the photovoltaic performance of **Z3**-based devices was very sensitive to the annealing process. With thermal annealing under 160 °C for 5 min, V_{oc}, J_{sc}, and FF of the **Z3**-based device were improved significantly. As a result, PCE of the device increased more than two times,

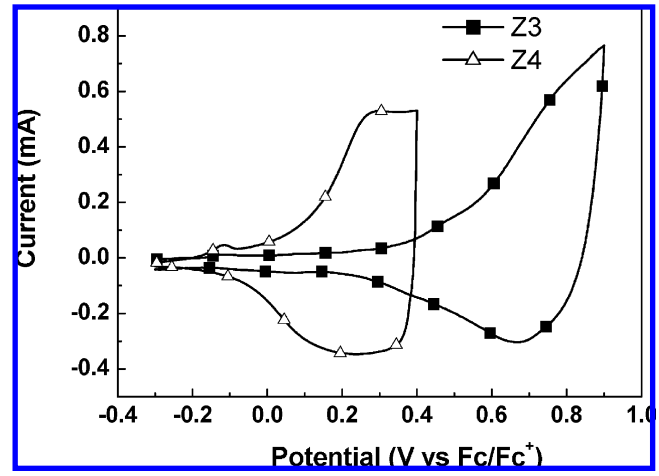

Figure 3. Cyclic voltammogram plots of **Z3** and **Z4**.

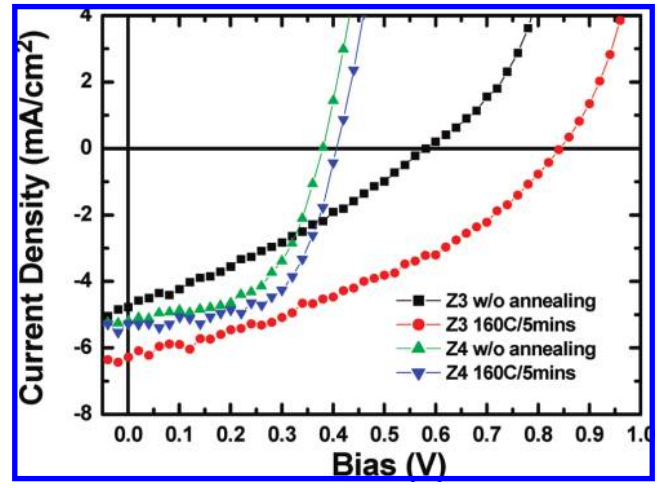

Figure 4. $I-V$ plots of the polymer solar cells based on **Z3** and **Z4**, with and without the annealing process.

from 0.85% to 1.95%. However, thermal treatment has little influence on **Z4**-based devices. After annealing, PCE of **Z4**-based devices slightly increased from 1.08% to 1.28%.

Absorption spectra of **Z3**:PCBM and **Z4**:PCBM composite films are shown in Figure 5a. The film preparation conditions of absorption measurements were kept the same as those in device fabrication for clear comparison. As shown in Figure 5a, the **Z4**:PCBM blend film exhibits a broader absorption band in comparison with the **Z3**:PCBM blend film. From their EQE curves in Figure 5b, it can be seen that the response range of **Z4**-based devices is also much broader than that of **Z3**-based devices; however, in the range from 350 to 600 nm, **Z3**-based devices exhibit better EQE than **Z4**-based devices, so J_{sc} of the **Z3**-based device is higher. Absorption spectra of the polymer:PCBM blend films have no change after annealing, but EQE of two kinds of devices increased obviously.

As shown in Table 2, although FF of the **Z3**-based device increased from 30.7% to 36.9% after annealing, this value is much lower than that of the **Z4**-based device, which reached 60% after annealing. The difference in FF values indicates that the charge carrier transport property of the two kinds of devices could be different, so the space charge limit current (SCLC) method was used to determine the hole mobility of the polymer:PCBM composite films. As listed in Table 2, the hole mobility of **Z4**:PCBM blend films is about 2 orders of magnitude higher

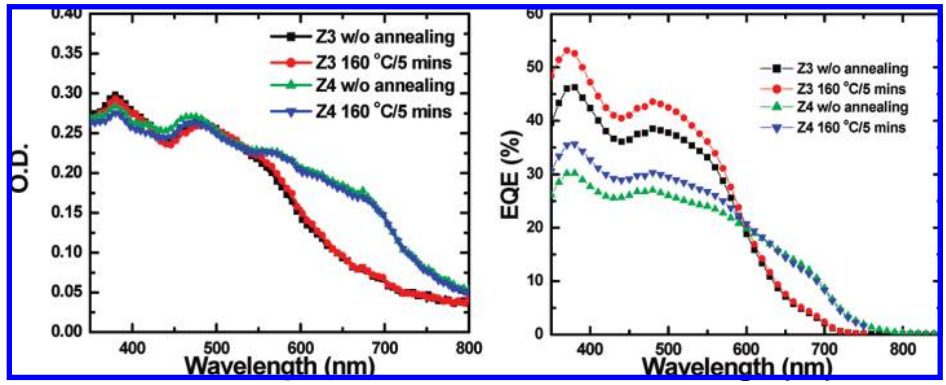

Figure 5. (a) Absorption spectra of **Z3**/PCBM and **Z4**/PCBM blend films, with and without the annealing process; (b) EQE curves of the polymer solar cells based on **Z3** and **Z4**, with and without the annealing process.

TABLE 2: Photovoltaic Results of the Polymer Solar Cells Based on Z3 and Z4

	V_{oc} (V)	J_{sc} (mA/cm^2)	PCE (%)	FF (%)	μ_h (cm^2/(V s))
Z3 w/o annealing	0.58	4.78	0.85	30.7	1.84×10^{-7}
Z3 160 °C/5 min	0.84	6.28	1.95	36.9	4.27×10^{-7}
Z4 w/o annealing	0.38	5.19	1.08	54.7	1.92×10^{-5}
Z4 160 °C/5 min	0.40	5.27	1.28	60.6	2.5×10^{-5}

than that of **Z3**:PCBM blend films, which should be the main reason for the better FF of **Z4**-based devices. As mentioned above, the interchain stacking of the adjacent main chains of **Z4** should be better than that of **Z3**, which might be the main reason that **Z4**:PCBM blend films exhibit much higher hole mobility than **Z3**:PCBM composite films.

Photoluminescence of the Polymer:PCBM Blends. Photoluminescence (PL) quenching provides direct evidence for exciton dissociation, and thus efficient PL quenching is necessary to obtain efficient organic solar cells. However, this does not necessarily mean that the stronger the PL quenching, the better the performance of the solar cells. In the P3HT/PCBM photovoltaic system, by using the solvent annealing process, the PL quenching effect of PCBM was weakened, but photovoltaic performance of the device was improved distinctly.[17] Since behaviors of **Z3**- and **Z4**-based solar cells are different under the annealing process, it is necessary to investigate the PL quenching effect of the two polymers. As shown in Figure 6, **Z3**:PCBM and **Z4**:PCBM blend films exhibited much different PL quenching effects after annealing. For the **Z4**:PCBM blend film, the luminescence spectra have no change after the annealing process. However, PL of the **Z3**:PCBM blend film was quenched by PCBM significantly before annealing and increased a lot after annealing. Although the comparison between these two kinds of blends provided qualitative results only, the phenomenon of PL enhanced by annealing indicates that aggregation of the polymer in the blend is likely increased during the annealing process, and as the surface between the polymer and PCBM phases is reduced, the PL of the polymer cannot be quenched thoroughly.[17] However, there is no clear exo- or endothermal process observed in the differential scanning calorimetry (DSC) measurement.

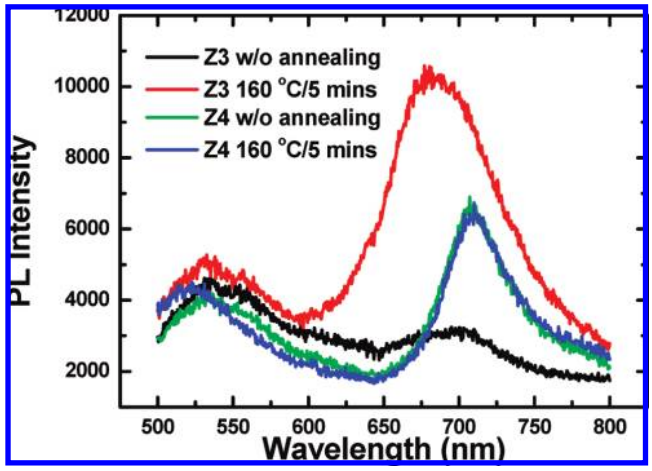

Figure 6. PL spectra of **Z3**/PCBM and **Z4**/PCBM blend films, without and with the annealing process.

Conclusion

Two BDT-based conjugated polymers, **Z3** and **Z4**, were designed and synthesized through a feasible approach. The hole mobility (μ_h) of **Z4** is 2 orders higher than that of **Z4**, due to the better planar structure of **Z4**. Photovoltaic results indicate that the **Z4**-based devices exhibited much higher FF values than the **Z3**-based devices, and also the **Z4**-based devices exhibited a broader response range than the **Z3**-based devices. Although, both bandgap and hole mobility of **Z4** are desirable as a photovoltaic material, its HOMO level is too high to obtain a good V_{oc}, due to the strong electron-donating effect of its alkyoxy groups. On the basis of these results, what we can conclude about molecular structure design of photovoltaic conjugated polymers is as follows: first, the steric hindrance between two adjacent units is an important issue, and second, to reduce the bandgap by adding electron-donating groups is not a favorable approach for photovoltaic conjugated polymers. After annealing, V_{oc} of the **Z3**-based device increased distinctly, from 0.58 to 0.84 V, and its FF also improved to 37%, and as a result, the efficiency of the device increased more than two times. However, the **Z4**-based device has little change after annealing. PL spectra indicate that PL intensity of the **Z3**:PCBM blend film increased after annealing, but PL of the **Z4**:PCBM blend film had no change after the annealing process, which indicates that the aggregation of polymer in the blend of **Z3**:PCBM is likely increased during the annealing process.

Experimental Section

Characterization. ^{1}H NMR spectra were measured on a Bruker DMX-400 spectrometer. Absorption spectra were taken with a Varian Cary 50 ultraviolet−visible spectrometer. The molecular weight of polymers was measured by the GPC method with chloroform as eluent, and polystyrene was used as a standard. The electrochemical cyclic voltammetry was conducted with a Pt disk coated with the polymer film, Pt wire, and Ag electrode as working electrode, counter electrode, and quasireference electrode, respectively, in a 0.1 mol/L of tetrabutylammonium hexafluorophosphate (Bu_4NPF_6) acetonitrile solution. Since Ag wire was used as a semireference electrode, a trace amount of ferrocene (Fc) was used as a standard material to determine the molecular energy level of the polymers. The thickness of the active layer of the polymer solar cell device was measured with a Dektak profilometer, and testing of the devices was done in a N_2-filled glovebox under AM 1.5G irradiation (100 mW cm^{-2}), using a Xenon lamp solar simulator calibrated with a silicon diode (with KG5 visible filter) calibrated with the assistance from the National Renewable Energy Laboratory (NREL).

Fabrication of PSC Devices. PSC devices with the typical structure of ITO/PEDOT-PSS/polymer:PCBM(1:3, w/w)/Ca/Al were fabricated under similar conditions as follows: After spin-coating a 30 nm layer of poly(3,4-ethylene dioxythiophene): poly(styrenesulfonate) onto a precleaned indium−tin oxide (ITO)-coated glass substrate, the polymer/PCBM blend solution was spin-coated. The typical concentration of the polymer/PCBM(1:3, w/w) blend solution used in this study for the spin-coating active layer was 10 mg/mL, and chlorobenezene was used as solvent. The thickness of the active layer was ∼70 nm. The devices were completed by evaporating Ca/Al metal electrodes with area of 10.5 mm^2 defined by masks.

Synthesis. ***4,8-Bis(2-ethylhexyloxy)benzo[1,2-b:3,4-b]dithiophene,*** **1.** 4,8-Dihydrobenzo[1,2-*b*:4,5-*b*′]dithiophen-4,8-dion (4.4 g, 20 mmol), zinc powder (2.86 g, 44 mmol), and 60 mL of water were put into a 250 mL flask, then 12 g of NaOH was added into the mixture. The mixture was well stirred and heated to reflux for 1 h. Then, 1-bromo-2-ethylhexane (11.6 g, 60 mmol) and a catalytic amount of tetrabutylammonium bromide were added into the flask, and the reactant was heated to reflux for 6 h. Then, the reactant was poured into cold water and extracted by 200 mL of diethyl ether two times. The ether layer was dried over anhydrous $MgSO_4$. After solvent was removed, the crude product was purified by silica gel chromatography, using hexane as eluent. A yield of 6.35 g of compound **4** (16.6 mmol, yield 71%) was obtained as a colorless sticky oil. ^{1}H NMR ($CDCl_3$, 400 MHz) δ (ppm) 7.67 (d, 2H), 7.37 (d, 2H), 4.19 (d, 4H), 1.7 (m, 2H), 1.6−1.4 (m, 16H), 1.08 (t, 6H), 0.92 (t, 6H). Elemental Anal. Calcd for $C_{26}H_{38}O_2S_2$: C, 69.91; H, 8.57. Found: C, 69.71; H, 8.45.

2,6-Dibromo-4,8-bis(2-ethylhexyl)benzo[1,2-b:3,4-b]dithiophene, **2.** Compound **1** (4.47 g, 10 mmol) was solved into 100 mL of methylene chloride in a 250 mL flask. Bromine (3.2 g, 20 mmol) was solved into 60 mL of methylene chloride in a funnel and slowly dropped into the flask under an ice−water bath, and then the reactant was stirred for 4−6 h at ambient temperature. When the color of the bromine was diminished, all of the volatile substances were removed under vacuum. The residue was purified by silica gel chromatography with hexane as eluent. A yield of 5.44 g of 2,6-dibromo-4,8-didodecyloxybenzo[1,2-*b*:3,4-*b*]dithiophene (9.0 mmol, yield 90%), compound **2**, was obtained as a colorless or pale yellow sticky oil. ^{1}H NMR ($CDCl_3$, 400 MHz) δ (ppm) 7.42 (s, 2H), 4.12 (d, 4H), 1.77 (m, 2H), 1.54−1.36 (m, 16H), 1.02 (t, 6H), 0.96 (t, 6H). Elemental Anal. Calcd for $C_{26}H_{36}Br_2O_2S_2$: C, 51.66; H, 6.00. Found: C, 51.23; H, 6.10.

2,6-Bis(trimethyltin)-4,8-bis(2-ethylhexyl)benzo[1,2-b:3,4-b′]dithiophene, **3.** Compound **2** (3.61 g, 6 mmol) and 60 mL of THF were added into a flask under inert atmosphere. The solution was cooled to −78 °C by a liquid nitrogen−acetone bath, and 4.55 mL of *n*-butyllithium (13.2 mmol, 2.9 M in *n*-hexane) was added. After the solution was stirred at −78 °C for 30 min, a great deal of white solid precipitate appeared in the flask. Then, 15 mmol of trimethyltin chloride (14 mL, 1 M in *n*-hexane) was added in one portion, and the reactant turned clear rapidly. The cooling bath was removed, and the reactant was stirred at ambient temperature for 2 h. Then, it was poured into 200 mL of cool water and extracted by ether 3 times. The organic layer was washed by water two times, and then dried by anhydrous $MgSO_4$. After the solvent was removed under vacuum, the residue was recrystallized by ethyl alcohol very carefully. A yield of 3.2 g of compound **3** (4.08 mmol, yield 68%) was obtained as a colorless needle crystal. ^{1}H NMR ($CDCl_3$, 400 MHz) δ (ppm) 7.52 (s, 2H), 4.23 (d, 4H), 1.79 (m, 2H), 1.54−1.36 (m, 16H), 1.06 (t, 6H), 0.96 (t, 6H), 0.40 (s, 18H). ^{13}C NMR ($CDCl_3$, 100 MHz) δ (ppm) 143.3, 140.4, 133.9, 132.9, 128.0, 75.7, 40.7, 30.6, 29.3, 23.9, 23.2, 14.2, 11.4, −8.3. Elemental Anal. Calcd for $C_{32}H_{54}O_2S_2Sn_2$: C, 49.76; H, 7.05. Found: C, 49.56; H, 7.12.

4,7-Bis(3-hexylthiophen-2-yl)-2,1,3-benzothiadiazole, **4.** 3-Hexylthiophene that was prepared by a reported method[18] (10 mmol, 1.68 g) was put into a flask with 20 mL of THF under an inert atmosphere. The solution was cooled to −78 °C by a liquid nitrogen−acetone bath, and 3.8 mL of *n*-butyllithium (11 mmol, 2.9 M in *n*-hexane) was added. The reactant was warmed to ambient temperature gradually and stirred at ambient temperature for an hour, and then tributylstannyl chloride (4.5 g, 14 mmol) was added in one portion. The reactant was stirred for an additional 2 h, and then extracted by diethyl ether. After removing solvent under vacuum, the residue, 2-(tributylstannyl)thiophene, was used directly for the Stille coupling reaction. 2-(Tributylstannyl)thiophene, 3 mmol of 4,7-dibromo-2,1,3-benzothiadiazole (0.88 g) prepared by a reported method,[19] and 30 mL of toluene were put into a flask. The solution was flushed with argon for 10 min, then 50 mg of $Pd(PPh_3)_4$ was added. The solution was flushed again for 20 min. The oil bath was heated to 110 °C, and the reactant was stirred for 16 h at this temperature under argon atmosphere. Then, the reactant was cooled to room temperature and extracted by diethyl ether several times. After solvent was removed, the crude product was purified by silica gel chromatography with hexane/methylene chloride (4:1; v/v) as eluent. The target compound, 0.94 g of 4,7-bis(3-hexylthiophen-2-yl)2,1,3-benzothiadiazole (2.0 mmol, 66%), was obtained as a yellow-orange oil. ^{1}H NMR ($CDCl_3$, 400 MHz) δ (ppm) 7.73 (s, 2H), 7.36 (d, 2H), 6.98 (d, 2H), 2.62 (t, 4H), 1.59 (m, 4H), 1.22 (m, 12H), 0.83 (t, 6H). ^{13}C NMR ($CDCl_3$, 100 MHz) δ (ppm) 154.2, 138.3, 132.4, 129.6, 127.5, 126.1, 124.2, 34.3, 31.8, 29.7, 24.6, 22.2, 14.1. Elemental Anal. Calcd for $C_{26}H_{32}N_2S_3$: C, 66.62; H, 6.88, N, 6.23. Found: C, 65.62; H, 6.47; N, 5.88.

4,7-Bis(5-bromo-3-hexylthiophen-2-yl)-2,1,3-benzothiadiazole, **5.** Compound **4** (0.94 g, 2 mmol) was solved into 30 mL of chloroform, and 0.712 g of NBS (4 mmol) was added in small portions. The reactant was stirred at ambient temperature overnight. Then, the reactant was extracted by chloroform several times. After solvent was removed under vacuum, the crude product was purified by silica gel chromatography with

hexane/methylene chloride (6:1; v/v) as eluent. A yield of 0.82 g of compound **5** (1.3 mmol, yield 65%) was obtained as an orange oil. ^{1}H NMR ($CDCl_3$, 400 MHz) δ (ppm) 7.64 (s, 2H), 6.97 (s, 2H), 2.68 (t, 4H), 1.57 (m, 4H), 1.22 (m, 12H), 0.83 (t, 6H). ^{13}C NMR ($CDCl_3$, 100 MHz) δ (ppm) 154.4, 139.3, 131.4, 133.6, 129.8, 129.6, 114.5, 34.3, 31.9, 30.0, 23.9, 21.9, 14.0. Elemental Anal. Calcd for $C_{26}H_{30}N_2S_3Br_2$: C, 49.84; H, 4.83; N, 4.67. Found: C, 49.44; H, 4.78; N, 4.56.

***4,7-Bis(3-hexyloxythiophen-2-yl)-2,1,3-benzothiadiazole,* 6.** The same synthetic procedure of compound **4** was used to prepare compound **6**, except that 3-hexyloxythiophene (10 mmol, 1.84 g) prepared by a reported method[20] was used instead of 3-hexylthiophene. The target product was purified by recrystallization, using ethanol as solvent, and 1.1 g of compound **6** (2.2 mmol) was obtained as red crystals (yield 73%). ^{1}H NMR ($CDCl_3$, 400 MHz) δ (ppm) 8.32 (s, 2H), 7.36 (d, 2H), 6.54 (d, 2H), 4.29 (t, 4H), 1.86 (m, 4H), 1.54 (m, 4H), 1.36 (m, 12H), 0.89 (t, 6H). Elemental Anal. Calcd for $C_{26}H_{32}N_2S_3O_2$: C, 62.36; H, 6.24; N, 5.89. Found: C, 62.11; H, 6.34; N, 5.49.

***4,7-Bis(5-bromo-3-hexyloxythiophen-2-yl)-2,1,3-benzothiadiazole,* 7.** NBS (0.72 g, 4 mmol) was slowly added to compound **6** (1.0 g, 2 mmol) in 15 mL of chloroform at 4 °C. The reactant was stirred for 1 h under that temperature, and then the cooling bath was removed. The reactant was warmed to room temperature and stirred overnight. After adding 50 mL of methanol to the reactant, the crude product was precipitated and filtered. The red precipitate was collected and purified by recrystallization with ethanol as solvent, and gave compound **7** with a yield of 66%. ^{1}H NMR ($CDCl_3$, 400 MHz) δ (ppm) 8.41 (s, 2H), 6.97 (d, 2H), 4.15 (t, 4H), 1.83 (m, 4H), 1.53 (m, 4H), 1.36 (m, 12H), 0.90 (t, 6H). ^{13}C NMR ($CDCl_3$, 100 MHz) δ (ppm) 160.7, 157.2, 132.0, 129.7, 124.3, 116.8, 120.2, 72.1, 34.2, 30.1, 26.3, 22.9, 14.2. Elemental Anal. Calcd for $C_{26}H_{30}N_2S_3O_2Br_2$: C, 47.42; H, 4.59; N, 4.83. Found: C, 47.33; H, 4.66; N, 4.65.

Polymerization of* Z3 *and* Z4 *by the Stille Coupling Reaction. In a 150 mL flask, compound **3** (0.74 g, 1 mmol) and compound **5** (0.627 g, 1 mmol) were dissolved into 50 mL of toluene, and flushed with argon for 10 min. Then, 22 mg of $Pd(PPh_3)_4$ was added into the flask, which was then flashed by argon for another 20 min. The solution was heated to reflux and stirred for 24 h under inert atmosphere. Then, the reactant was cooled to room temperature, and the polymer was precipitated by addition of 50 mL of methanol and filtered through a Soxhlet thimble, which was then subjected to Soxhlet extraction with methanol, hexane, and chloroform. The polymer was recovered as a solid sample from the chloroform fraction by rotary evaporation. The deep red solid was dried under vacuum for 1 day to obtain the final product **Z3** (490 mg, yield 46%). ^{1}H NMR ($CDCl_3$, 400 MHz) δ (ppm) 8.35 (s, 2H), 6.8 (broad, 4H), 4.1 (broad, 4H), 2.8−1.3 (broad, 38H), 1.1−0.8 (broad, 18H). Elemental Anal. Calcd for $C_{52}H_{66}N_2O_2S_5$: C, 68.53; H, 7.30; N, 3.07. Found: C, 66.90; H, 6.91; N, 3.17.

Polymer **Z4** was synthesized by the same procedure as **Z3**. Compound **6** (0.659 g, 1 mmol) was used instead of compound **5**, and **Z4** was obtained as a dark powder (684 mg, yield 62%). ^{1}H NMR ($CDCl_3$, 400 MHz) δ (ppm) 8.4 (s, 2H), 6.9 (broad, 4H), 4.2 (broad, 8H), 2.0−1.76 (broad, 6H), 1.6−1.3 (m, 28H), 1.1−0.8 (broad, 18H). Elemental Anal. Calcd for $C_{52}H_{66}N_2O_4S_5$: C, 66.20; H, 7.05; N, 2.97. Found: C, 65.80; H, 7.23; N, 3.02.

Acknowledgment. .

This work was financially supported by Solarmer Energy Inc., UC Discovery Grant (Grant No. GCP05-10208).

References and Notes

(1) Sariciftci, N. S.; Smilowitz, L.; Heeger, A. J.; Wudl, F. *Science* **1992**, *258*, 1474.

(2) Gunes, S.; Neugebauer, H.; Sariciftci, N. S. *Chem. Rev.* **2007**, *107*, 1324.

(3) Kim, J. Y.; Lee, K.; Coates, N. E.; Moses, D.; Nguyen, T.-Q.; Dante, M.; Heeger, A. J. *Science* **2007**, *317*, 222.

(4) Coakley, K. M.; McGehee, M. D. *Chem. Mater.* **2004**, *16*, 4533.

(5) Brabec, J.; Sariciftci, N. S.; Hummelen, J. C. *Adv. Funct. Mater.* **2001**, *11*, 15.

(6) Li, G.; Shrotriya, V.; Huang, J.; Yao, Y.; Moriarty, T.; Emery, K.; Yang, Y. *Nat. Mater.* **2005**, *4*, 865.

(7) (a) Winder, C.; Sariciftci, N. S. *J. Mater. Chem.* **2004**, *14*, 1077. (b) Hou, J.; Tan, Z.; Yan, Y.; He, Y.; Yang, C.; Li, Y. *J. Am. Chem. Soc.* **2006**, *128*, 4911. (c) Hou, J.; Chen, H. Y.; Zhang, S.; Li, G.; Yang, Y. *J. Am. Chem. Soc.* **2008**, *130*, 16144.

(8) (a) Scharber, M. C.; Mühlbacher, D.; Koppe, M.; Denk, P.; Waldauf, C.; Heeger, A. J.; Brabec, C. J. *Adv. Mater.* **2006**, *18*, 789. (b) Blouin, N.; Michaud, A.; Gendron, D.; Wakim, S.; Blair, E.; Neagu-Plesu, R.; Belletete, M.; Durocher, G.; Tao, Y.; Leclerc, M. *J. Am. Chem. Soc.* **2008**, *130*, 732.

(9) Liang, Y.; Feng, D.; Wu, Y.; Tsai, S.; Li, G.; Ray, C.; Yu, L. *J. Am. Chem. Soc.* **2009**, *131*, 7792.

(10) Wang, E.; Wang, L.; Lan, L.; Luo, C.; Zhuang, W.; Peng, J.; Cao, Y. *Appl. Phys. Lett.* **2008**, *92*, 033307.

(11) Thompson, B. C.; Kim, Y. G.; Reynolds, J. R. *Macromolecules* **2005**, *38*, 5359.

(12) Koster, L. J. A.; Mihailetchi, V. D.; Blom, P. W. M. *Appl. Phys. Lett.* **2006**, *88*, 093511.

(13) Hou, J.; Park, M.-H.; Zhang, S.; Yao, Y.; Chen, L.-M.; Li, J.-H.; Yang, Y. *Macromolecules.* **2008**, *41*, 6012.

(14) Goedel, W. A.; Somanathan, N. S.; Enkelmann, V.; Wegner, G. *Makromol. Chem.* **1992**, *193*, 1195.

(15) Somanathan, N.; Radhakrishnan, S. *Int. J. Mod. Phys. B* **2005**, *19*, 4645.

(16) Li, Y. F.; Cao, Y.; Gao, J.; Wang, D. L.; Yu, G.; Heeger, A. J. *Synth. Met.* **1999**, *99*, 243.

(17) Li, G.; Yao, Y.; Yang, H.; Shrotriya, V.; Yang, G.; Yang, Y. *Adv. Funct. Mater.* **2007**, *17*, 1636.

(18) Pham, C. V.; Mark, H. B.; Zimmer, H. *Synth. Commun.* **1986**, *16*, 689.

(19) Pilgram, K.; Zupan, M.; Skiles, R. *J. Heterocycl. Chem.* **1970**, *7*, 629.

(20) Zhou, L.; Jin, S.; Xue, G. *Synth. Commun.* **1996**, *26*, 3725.

JP9060413